# Gas-Phase Reactions of Brominated Diphenyl Ethers with OH Radicals

**Jonathan D. Raff and Ronald A. Hites***

*School of Public and Environmental Affairs, Indiana University, Bloomington, Indiana 47405*

*Received: May 17, 2006; In Final Form: July 7, 2006*

A small volume reaction chamber coupled to a mass spectrometer was used to study the gas-phase kinetics and mechanism of the reaction of OH radicals with diphenyl ether and seven polybrominated diphenyl ethers (PBDEs) with 1−2 bromines. Relative rate constants for these reactions were determined using isopropyl nitrite photolysis in He−air mixtures at ∼740 Torr between the temperatures of 326−388 K. The Arrhenius expression for each compound was used to extrapolate the following OH rate constants at 298 K (in units of $10^{-12}$ cm$^3$ molecule$^{-1}$ s$^{-1}$, with 95% confidence intervals): diphenyl ether, 7.45 ± 0.13; 2-bromodiphenyl ether, $4.70^{+0.53}_{-0.48}$; 3-bromodiphenyl ether, $4.60^{+0.70}_{-0.61}$; 4-bromodiphenyl ether, $5.75^{+0.42}_{-0.39}$; 2,2′-dibromodiphenyl ether, $1.33^{+0.31}_{-0.25}$; 2,4-dibromodiphenyl ether, $3.88^{+0.87}_{-0.71}$; 3,3-dibromodiphenyl ether, $3.23^{+0.70}_{-0.57}$; and 4,4′-bromodiphenyl ether, $5.14^{+0.98}_{-0.82}$. The measured OH rate constants are in reasonable agreement with those predicted by structure activity relationships. Positive temperature dependences of these OH rate constants are observed for all compounds measured except for diphenyl ether and 4,4′-dibromodiphenyl ether. Bromophenols (in yields up to 20% relative to the amount of PBDE consumed) and $Br_2$ were characterized as products of these reactions, suggesting that OH addition to ipso positions of these brominated aryls may be an important reaction pathway.

## Introduction

Polybrominated diphenyl ethers (PBDEs) have become widespread global pollutants due to their heavy use (∼70 000 metric tons sold in 2003) as flame-retardants in polyurethane foam and in synthetic commercial fibers.[1] These semivolatile compounds have between 2 and 10 bromine substituents and undergo long-range atmospheric transport[2,3] to remote regions such as the Arctic Circle, where they enter food chains and biomagnify in top predators.[4,5] PBDE concentrations have increased exponentially in the environment, and it is estimated that PBDEs may soon surpass polychlorinated biphenyls (PCBs) as the most prevalent persistent organic pollutants in the Canadian Arctic.[5] Chronic exposure to these chemicals may pose a serious threat to wildlife and humans since PBDEs and their metabolites are considered to be potential endocrine disruptors.[6]

Despite efforts to characterize the extent of PBDE contamination in the environment, little is known about the atmospheric chemistry that PBDEs undergo during long-range atmospheric transport. Such information is essential for accurate predictions regarding persistence and health threats from exposure to PBDEs and their potentially harmful degradation products.

Similar to other aromatic hydrocarbons, both gas- and particle-phase PBDEs are expected to undergo photolysis and reactions with atmospheric oxidants, such as hydroxyl (OH) and nitrate ($NO_3$) radicals and $O_3$.[7] The photolytic degradation of PBDEs has been studied with an emphasis on solution and mixed-phase processes,[8−13] and reductive debromination has been shown to occur in solution with photolysis half-lives ranging from less than 1 h to more than a year, depending on the congener, the solvent, and the quenching characteristics of cosolutes and substrates.[8−13] In a smog chamber experiment, Zetzsch and co-workers[13] determined a rate constant for the reaction of OH with 2,2′,4,4′,5,5′-hexabromodiphenyl ether bound to silica that was eight times higher than the structure−activity relationship (SAR) prediction.[14,15] At present, the origin of this discrepancy remains unclear. There are no experimental data available on the rate constants for the gas-phase reactions of PBDEs with OH radicals, although the above evidence suggests that such reactions may be important loss processes for PBDEs in the atmosphere.

The goal of the present work is to determine the rate constants for the gas-phase reactions of OH with PBDEs using a small volume reaction chamber coupled to a mass spectrometer. With this experimental approach, the relative rate constants of semivolatile organic compounds are measured at temperatures such that their vapor pressures within the reactor are high enough to allow for detection by an online mass spectrometer.[16] Room-temperature rate constants for semivolatile organic compounds with vapor pressures as low as $10^{-4}$−$10^{-5}$ Torr are determined by extrapolation from Arrhenius plots.[17−19] In this study, the rate constants as a function of temperature and the atmospheric lifetimes of eight PBDEs containing 0−2 bromines have been calculated at 298 K and compared with predictions based on their structure−OH reactivity relationship. These results are applicable for understanding the atmospheric reactivity of those PBDEs found in the gas phase (i.e., congeners with fewer than six bromines). Several products of the OH−BDE reaction are reported, and the atmospheric implications of our findings are discussed.

## Experimental Section

Reactions were performed in 160 cm$^3$ quartz reaction chambers located in the oven of a Hewlett-Packard 5890 gas

* To whom correspondence should be addressed. E-mail: HitesR@Indiana.edu.

10.1021/jp0630222 CCC: $33.50 © 2006 American Chemical Society
Published on Web 08/24/2006

**TABLE 1: Ions of Reactants and Reference Compounds Monitored by Electron Impact Mass Spectrometry during Kinetic Experiments**

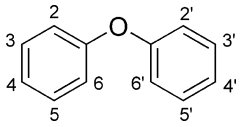


| compound | *m*/*z* values and their assignment |
|---|---|
| diphenyl ether | 170 $[M]^+$, 141 $[M - HCO]^+$ |
| 2-bromodiphenyl ether (BDE-1) | 248 $[M]^+$, 250 $[M + 2]^+$, 141 $[M - COBr]^+$ |
| 3-bromodiphenyl ether (BDE-2) | 248 $[M]^+$, 250 $[M + 2]^+$, 141 $[M - COBr]^+$ |
| 4-bromodiphenyl ether (BDE-3) | 248 $[M]^+$, 250 $[M + 2]^+$, 141 $[M - COBr]^+$ |
| 2,2′-dibromodiphenyl ether (BDE-4) | 326 $[M]^+$, 328 $[M + 2]^+$, 330 $[M + 4]^+$, 168 $[M - Br_2]^+$ |
| 2,4-dibromodiphenyl ether (BDE-7) | 328 $[M + 2]^+$, 168 $[M - Br_2]^+$ |
| 3,3′-dibromodiphenyl ether (BDE-11) | 326 $[M]^+$, 328 $[M + 2]^+$, 330 $[M + 4]^+$, 168 $[M - Br_2]^+$ |
| 4,4′-dibromodiphenyl ether (BDE-15) | 328 $[M + 2]^+$, 168 $[M - Br_2]^+$ |
| biphenyl | 154 $[M]^+$, 153 $[M - H]^+$ |
| fluorene | 166 $[M]^+$, 165 $[M - H]^+$ |
| 3-chlorobiphenyl (PCB-2) | 188 $[M]^+$, 152 $[M - HCl]^+$ |
| hexafluoropropene ($C_3F_6$) | 150 $[M]^+$, 131 $[M - F]^+$, 100 $[M - CF_2]^+$ |

chromatograph (for temperature control) and interfaced to a Hewlett-Packard 5989A quadrupole mass spectrometer (MS) operated in the electron impact (EI) mode.[20] Reactions were studied in a gas mixture of air and helium (1:4 v/v) under static conditions at about 740 Torr. The previously described apparatus was modified as follows: The reactor was coupled to the ion source by a shorter transfer line (45 cm long) made from a 0.28 mm inner diameter (i.d.) methyl-deactivated stainless steel capillary (MXT Hydroguard, Restek) heated at 150 °C; the light source was a 200 W Xe−Hg arc lamp (Hamamatsu Corporation); the broad-band spectrum of the lamp was filtered by a dichroic mirror (Hamamatsu Corporation) to eliminate IR and a BG-40 edge filter (Andover Corporation) to eliminate wavelengths less than 320 nm; and the light was collimated to a 5 cm diameter beam with an f/1.0 condensing lens (Newport) before entering the reactor.

Hydroxyl radicals were generated by irradiation (1−5 min) of isopropyl nitrite (*i*-$C_3H_7ONO$) at wavelengths above 320 nm

$$i\text{-}C_3H_7ONO + h\nu \rightarrow i\text{-}C_3H_7O + NO \quad (1)$$

$$i\text{-}C_3H_7O + O_2 \rightarrow CH_3C(O)CH_3 + HO_2 \quad (2)$$

$$HO_2 + NO \rightarrow OH + NO_2 \quad (3)$$

Initial attempts to measure relative rate constants using methyl nitrite photolysis as an OH source failed due to the formation of formaldehyde, which effectively scavenged OH in the reaction chamber, resulting in unreasonably slow decays in the PBDE and reference compound signals. Acetone is a byproduct of isopropyl nitrite photolysis, and the OH reactivity of acetone is considerably lower than that of the PBDEs and reference compounds studied here. The photolysis of hydrogen peroxide/He mixtures at $\lambda \geq 320$ nm was also investigated as a source of OH radicals in these kinetic experiments. At higher wavelengths, this is a very weak source of OH radicals and could not produce the high OH concentrations required to react with PBDEs on a reasonable time scale. Hydrogen peroxide was used in several product studies where the low OH concentrations generated proved useful in reducing secondary reactions with the OH + PBDE products.

**Kinetic Experiments.** A relative rate method was used to measure the rate constants of diphenyl ether and several PBDEs with OH radicals; the compounds studied are shown in Table 1. In the case of semivolatile organic compounds, it is assumed that the only removal processes in the reactor are reactions with OH or adsorption onto the reactor walls leading to permanent removal from the gas phase on the time scale of the experiments (reactions 4−7).

$$\text{PBDE} + \text{OH} \xrightarrow{k_4} \text{products} \quad (4)$$

$$\text{PBDE} + \text{wall} \xrightarrow{k_5} \text{wall loss} \quad (5)$$

$$\text{reference compound} + \text{OH} \xrightarrow{k_6} \text{products} \quad (6)$$

$$\text{reference compound} + \text{wall} \xrightarrow{k_7} \text{wall loss} \quad (7)$$

The values of $k_5$ and $k_7$ are obtained from a first-order exponential fit to the decay of the PBDE and reference compound signals 10 min prior to their reaction with OH radicals. During UV irradiation of the reactor, the intensities of *m*/*z* values belonging to the test and reference compounds follow the relationship

$$\ln\frac{[\text{PBDE}]_0}{[\text{PBDE}]_t} - k_5 t = \frac{k_4}{k_6}\left(\ln\frac{[\text{reference compound}]_0}{[\text{reference compound}]_t} - k_7 t\right) \quad (8)$$

where the signal intensities are measured at time $t = 0$ and at subsequent times, $t$. Wall losses of the PBDE and reference compound are accounted for by the terms $k_5 t$ and $k_7 t$, respectively. The slope of the plot of $\ln([\text{reference compound}]_0/[\text{reference compound}]_t) - k_7 t$ vs $\ln([\text{PBDE}]_0/[\text{PBDE}]_t) - k_5 t$ provides the ratio of the rate constants of the two simultaneous reactions. The independently determined rate constant of the reference compound is multiplied by the value of this ratio to derive the rate constant of the PBDE, $k_4$.

In a typical experiment, approximately 0.4−2 mL of *i*-$C_3H_7ONO$ vapor was introduced into the reaction chamber using a gastight syringe (Hamilton Co.). The isopropyl nitrite was stored as a solid under vacuum in a Schlenk tube and allowed to attain room temperature when it was necessary to transfer vapor to the reactor. Between 0.25 and 6 $\mu$g of a selected PBDE and reference compound were subsequently added to achieve identical instrument responses for the most intense *m*/*z* values monitored; solid and liquid PBDEs or reference compounds were added as $CCl_4$ solutions, and $C_3F_6$ was added as a gas using a gastight syringe. The steady-state concentration of OH in the reaction chamber was $0.2-1 \times 10^9$ molecules $cm^{-3}$, as

calculated from the decay rate of the reference compound, according to

$$[\mathrm{OH}] = \frac{1}{k_6 t}\left(\ln \frac{[\text{reference compound}]_0}{[\text{reference compound}]_t} - k_7 t\right) \qquad (9)$$

Reference compounds were chosen based on a variety of selection criteria that have been discussed in detail elsewhere.[20] It was often difficult to find reference compounds whose *m*/*z* values did not overlap with those of the PBDEs studied. This was due, in part, to the nonchromatographic MS inlet and the tendency of diphenyl ether analogues to fragment over a wide mass range upon electron impact. Suitable reference compounds were as follows: biphenyl, 3-chlorobiphenyl (PCB-2), hexafluoropropene ($C_3F_6$), and fluorene; specific *m*/*z* values monitored for reference and test compounds are listed in Table 1. The mass spectrometric response of each compound was linear over the range of concentrations used in this study. Rate constants of the reference compounds ($k_6$) are from Calvert et al.[7,21] (for biphenyl and fluorene) or from previously measured Arrhenius parameters.[17,22]

**Product Studies.** Products arising from the OH + PBDE reactions were identified using online and offline analysis of the reactor containing He/air mixtures at ~740 Torr and 70 °C. Online analysis of the reaction cell contents, using full scan (*m*/*z* 125−300) electron impact mass spectrometry, was used to follow the loss of reactants and the generation of products during OH reactions as a function of time. For offline analysis, 2.5 $\mu$g of a PBDE (in $CCl_4$) was introduced into the reactor containing either 12 $\mu$L of $H_2O_2$ (introduced as a liquid) or 0.4 $\mu$L of *i*-$C_3H_7ONO$ vapor. After a 30 min irradiation ($\lambda \geq 320$ nm), the reactor was cooled to −10 °C to condense semivolatiles to the reactor walls, removed from the instrument, and rinsed several times with a total of 8 mL of 1:1 (v/v) methyl *tert*-butyl ether and dichloromethane. The extracts were dried with $Na_2SO_4$, reduced in volume to ~200 $\mu$L with a gentle stream of $N_2$, and either analyzed directly by gas chromatographic mass spectrometry (GC/MS) operated in electron impact mode or derivitized with diazomethane (generated from the reaction of *N*-methyl-*N*-nitroso-*p*-toluenesulfonamide with KOH)[23] prior to GC/MS analysis. Chromatographic separation was achieved with an Agilent 6890 gas chromatograph fitted with a 30 m × 250 $\mu$m i.d. DB-5MS column (J&W Scientific) using He as the carrier gas (oven temperature program: 40 °C held for 2 min., 40−100 °C at 5 °C min$^{-1}$, 100−105 °C at 2 °C min$^{-1}$, 105−300 °C at 30 °C min$^{-1}$ with a 10 min hold). The detector used was an Agilent 5973 quadrupole mass spectrometer.

**Chemicals.** 3-Chlorobiphenyl and all brominated diphenyl ethers were obtained from Accustandard (New Haven, CT) as liquids or solids (>99%). Brominated phenols (>99%) were obtained from Cambridge Isotope laboratories, Inc. (Andover, MA). Isopropyl nitrite (97%) was purchased from Pfaltz & Bauer (Waterbury, CT). *i*-$C_3H_7ONO$ was protected from light and subjected to repeated freeze−pump−thaw cycles prior to each experiment; when not used, it was stored under vacuum at −30 °C. Ultrahigh purity (99.999%) helium and ultrazero ambient monitoring air were purchased from Praxair, Inc. (Indianapolis, IN). All other reagents and solvents were obtained from Aldrich Chemical Co. (Milwaukee, WI) and used without further purification.

## Results and Discussion

**Characterization of Dark and Photolysis Reactions.** The dark decays (wall losses and dark reactions) of PBDEs in the reactor amount to between 3 and 15% of the loss rate due to reaction with OH radicals, depending on the temperature and vapor pressure of the reactant. Pre-reaction decay of reference compounds amounted to ≤8%, ≤5%, ≤2%, and ≤4% of the losses from reaction with OH radicals for biphenyl, 3-chlorobiphenyl (PCB-2), hexafluoropropene ($C_3F_6$), and fluorene, respectively.

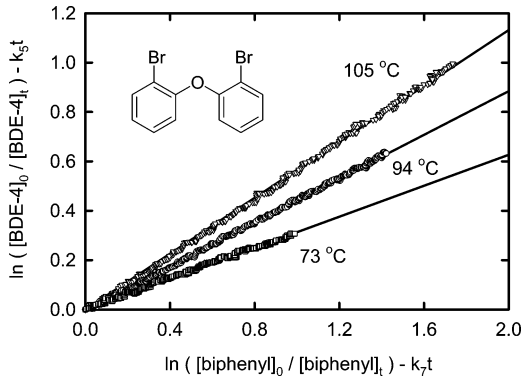


**Figure 1.** Plot of eq 8 for the gas-phase reaction of OH radicals with 2,2′-dibromodiphenyl ether (BDE-4) at three different temperatures, using biphenyl as the reference compound. The signals at *m*/*z* 168 and 154 were used for BDE-4 and biphenyl, respectively. The correlation coefficients ($r^2$) for the regressions at 73, 84, and 105 °C are 0.9961, 0.9990, and 0.9987, respectively.

Control experiments in the absence of *i*-$C_3H_7ONO$ indicated that photolysis of diphenyl ether derivatives and reference compounds did not occur under the conditions of the experiments; that is, the decay of the aromatic reactants under UV irradiation was indistinguishable from the wall losses observed in the dark. The reactor was purged with helium at 180 °C for 1 h between experiments, and a thoroughly cleaned reactor (rinsed with deionized water and baked at 450 °C for 12 h) was installed every 5−8 experiments. The lack of decay observed during the control experiments performed in the absence of *i*-$C_3H_7ONO$ indicated that these practices successfully prevented the accumulation of reactants and products and eliminated the heterogeneous formation of radicals that might interfere with the PBDE + OH kinetic measurements.

**Rate Constant Measurements.** A typical relative rate plot showing the loss of 2,2′-dibromodiphenyl ether vs that of the reference compound (biphenyl) in the presence of OH radicals at three different temperatures is shown in Figure 1. The relative rate plots for all diphenyl ether derivatives were constructed using data from the first 1−3 min of the reaction and are described by eq 8. Excellent linearity was observed for all relative rate plots within the temperature ranges studied, suggesting that secondary reactions were minimal. At a given temperature, each ratio was obtained by averaging the slopes of the relative rate plots for all combinations of PBDE and reference compound masses listed in Table 1. The rate constants and their ratios for the reaction of OH with diphenyl ether, three monobromodiphenyl ethers, and four dibromodiphenyl ethers are summarized in Table 2. Uncertainties in the rate constants do not include the error of the reference compound rate constants, which are estimated to be ±30%, ±20%, ±10%, and ±50% for biphenyl, PCB-2, $C_3F_6$, and fluorene, respectively. Arrhenius parameters were determined by a linear least-squares regression of the natural logarithms of the measured rate constants vs reciprocal absolute temperatures and are given in Table 3. Rate constants at 298 K were calculated from the Arrhenius parameters; these are given in Table 3 along with the 95% confidence intervals of the estimates.

**TABLE 2: Summary of Average Measured Rate Constant Ratios, $k_4/k_6$, and Rate Constants, $k_4$ ($10^{-12}$ cm$^3$ molecule$^{-1}$ s$^{-1}$), for the Gas-Phase Reactions of Diphenyl Ether and Mono- and Dibrominated Diphenyl Ethers with OH Radicals**

| $T$ (K) | ref. compd.[a] | $k_4/k_6$ | $k_4$[b] | $T$ (K) | ref. compd.[a] | $k_4/k_6$ | $k_4$[b] |
|---|---|---|---|---|---|---|---|
| | | | diphenyl ether | | | | |
| 326 | bp | 1.04 ± 0.15[b] | 7.35 ± 1.26 | 342 | bp | 1.06 ± 0.01 | 7.53 ± 0.05 |
| 326 | bp | 1.03 ± 0.04 | 7.28 ± 0.27 | 342 | bp | 1.05 ± 0.15 | 7.44 ± 1.09 |
| 326 | hfp | 3.87 ± 0.71 | 7.51 ± 1.37 | 346 | bp | 1.07 ± 0.04 | 7.61 ± 0.25 |
| 326 | hfp | 3.66 ± 0.71 | 7.10 ± 1.37 | 346 | bp | 1.10 ± 0.08 | 7.82 ± 0.57 |
| 331 | bp | 1.04 ± 0.09 | 7.38 ± 0.60 | 346 | hfp | 3.88 ± 0.10 | 7.20 ± 0.19 |
| 336 | hfp | 4.12 ± 0.47 | 7.63 ± 0.88 | 352 | bp | 1.05 ± 0.07 | 7.46 ± 0.48 |
| 336 | hfp | 3.79 ± 0.37 | 7.17 ± 0.70 | 357 | bp | 1.12 ± 0.04 | 7.93 ± 0.25 |
| 339 | bp | 1.08 ± 0.02 | 7.69 ± 0.14 | 367 | hfp | 4.02 ± 0.17 | 7.14 ± 0.31 |
| | | | 2-bromodiphenyl ether (BDE-1) | | | | |
| 326 | bp | 0.758 ± 0.077 | 5.38 ± 0.55 | 356 | f | 0.466 ± 0.039 | 6.52 ± 0.55 |
| 331 | bp | 0.793 ± 0.011 | 5.63 ± 0.08 | 357 | bp | 0.858 ± 0.038 | 6.09 ± 0.27 |
| 336 | bp | 0.858 ± 0.038 | 6.09 ± 0.27 | 367 | bp | 0.890 ± 0.019 | 6.32 ± 0.14 |
| 336 | bp | 0.788 ± 0.025 | 5.59 ± 0.18 | 367 | bp | 0.949 ± 0.021 | 6.74 ± 0.15 |
| 346 | bp | 0.809 ± 0.043 | 5.74 ± 0.31 | 367 | f | 0.477 ± 0.042 | 6.68 ± 0.59 |
| 346 | f | 0.446 ± 0.062 | 6.25 ± 0.86 | | | | |
| | | | 3-bromodiphenyl ether (BDE-2) | | | | |
| 326 | bp | 0.798 ± 0.019 | 5.67 ± 0.14 | 346 | pcb2 | 1.18 ± 0.07 | 6.43 ± 0.37 |
| 326 | pcb2 | 1.29 ± 0.03 | 6.75 ± 0.18 | 346 | bp | 0.988 ± 0.027 | 7.02 ± 0.19 |
| 326 | pcb2 | 1.07 ± 0.03 | 5.62 ± 0.16 | 351 | bp | 0.965 ± 0.060 | 6.85 ± 0.43 |
| 331 | pcb2 | 1.14 ± 0.12 | 6.03 ± 0.64 | 354 | pcb2 | 1.26 ± 0.12 | 6.97 ± 0.66 |
| 336 | pcb2 | 1.24 ± 0.15 | 6.62 ± 0.79 | 356 | bp | 1.12 ± 0.05 | 7.93 ± 0.39 |
| 336 | bp | 0.867 ± 0.030 | 6.15 ± 0.21 | 361 | bp | 1.09 ± 0.07 | 7.73 ± 0.52 |
| 341 | bp | 0.860 ± 0.063 | 6.11 ± 0.45 | 367 | bp | 1.15 ± 0.07 | 8.19 ± 0.50 |
| 346 | bp | 1.07 ± 0.12 | 7.62 ± 0.88 | 367 | pcb2 | 1.36 ± 0.04 | 7.65 ± 0.25 |
| | | | 4-bromodiphenyl ether (BDE-3) | | | | |
| 326 | bp | 0.864 ± 0.027 | 6.14 ± 0.19 | 347 | bp | 0.857 ± 0.065 | 6.09 ± 0.46 |
| 326 | bp | 0.860 ± 0.056 | 6.11 ± 0.40 | 357 | bp | 0.854 ± 0.087 | 5.90 ± 0.28 |
| 326 | bp | 0.797 ± 0.080 | 5.66 ± 0.57 | 357 | bp | 0.831 ± 0.040 | 5.97 ± 0.32 |
| 334 | bp | 0.858 ± 0.034 | 6.09 ± 0.24 | 368 | bp | 0.884 ± 0.051 | 6.28 ± 0.37 |
| 337 | bp | 0.811 ± 0.025 | 5.76 ± 0.18 | 368 | bp | 0.884 ± 0.042 | 6.28 ± 0.29 |
| 347 | bp | 0.869 ± 0.106 | 6.17 ± 0.75 | 368 | bp | 0.869 ± 0.056 | 6.17 ± 0.40 |
| | | | 2,2′-dibromodiphenyl ether (BDE-4) | | | | |
| 346 | pcb2 | 0.513 ± 0.006 | 2.79 ± 0.03 | 367 | pcb2 | 0.605 ± 0.118 | 3.41 ± 0.66 |
| 346 | bp | 0.362 ± 0.021 | 2.57 ± 0.15 | 367 | bp | 0.462 ± 0.027 | 3.28 ± 0.20 |
| 346 | bp | 0.361 ± 0.012 | 2.56 ± 0.09 | 378 | bp | 0.559 ± 0.065 | 3.98 ± 0.46 |
| 357 | bp | 0.425 ± 0.072 | 3.02 ± 0.51 | 378 | pcb2 | 0.626 ± 0.067 | 3.58 ± 0.38 |
| 357 | pcb2 | 0.588 ± 0.091 | 3.26 ± 0.50 | 378 | bp | 0.567 ± 0.091 | 4.03 ± 0.64 |
| 367 | bp | 0.466 ± 0.059 | 3.31 ± 0.42 | | | | |
| | | | 2,4-dibromodiphenyl ether (BDE-7) | | | | |
| 347 | bp | 0.681 ± 0.037 | 4.84 ± 0.26 | 369 | pcb2 | 0.965 ± 0.058 | 5.44 ± 0.33 |
| 347 | bp | 0.701 ± 0.091 | 4.98 ± 0.65 | 379 | bp | 0.720 ± 0.118 | 5.12 ± 0.84 |
| 347 | pcb2 | 0.884 ± 0.074 | 4.82 ± 0.40 | 379 | bp | 0.832 ± 0.069 | 5.91 ± 0.49 |
| 358 | bp | 0.759 ± 0.069 | 5.39 ± 0.49 | 379 | bp | 0.779 ± 0.029 | 5.53 ± 0.21 |
| 358 | pcb2 | 0.888 ± 0.098 | 4.93 ± 0.54 | 379 | pcb2 | 0.943 ± 0.136 | 5.39 ± 0.78 |
| 369 | bp | 0.805 ± 0.045 | 5.71 ± 0.32 | | | | |
| | | | 3,3′-dibromodiphenyl ether (BDE-11) | | | | |
| 346 | pcb2 | 0.931 ± 0.032 | 5.04 ± 0.17 | 367 | pcb2 | 1.05 ± 0.06 | 5.85 ± 0.31 |
| 346 | pcb2 | 0.976 ± 0.021 | 5.29 ± 0.11 | 367 | bp | 0.874 ± 0.027 | 6.21 ± 0.13 |
| 346 | bp | 0.721 ± 0.089 | 5.12 ± 0.45 | 378 | pcb2 | 1.13 ± 0.07 | 6.43 ± 0.40 |
| 357 | pcb2 | 0.934 ± 0.065 | 5.14 ± 0.36 | 378 | bp | 0.907 ± 0.049 | 6.44 ± 0.24 |
| 357 | bp | 0.742 ± 0.032 | 5.27 ± 0.16 | | | | |
| | | | 4,4′-dibromodiphenyl ether (BDE-15) | | | | |
| 357 | hfp | 2.10 ± 0.05 | 3.80 ± 0.10 | 378 | hfp | 2.07 ± 0.12 | 3.61 ± 0.21 |
| 357 | hfp | 2.09 ± 0.12 | 3.78 ± 0.22 | 378 | hfp | 2.05 ± 0.14 | 3.57 ± 0.24 |
| 357 | hfp | 2.08 ± 0.07 | 3.77 ± 0.12 | 386 | hfp | 2.00 ± 0.05 | 3.43 ± 0.08 |
| 357 | hfp | 2.24 ± 0.09 | 4.06 ± 0.16 | 386 | hfp | 1.91 ± 0.05 | 3.27 ± 0.09 |
| 367 | hfp | 2.11 ± 0.09 | 3.75 ± 0.16 | 388 | hfp | 2.12 ± 0.11 | 3.63 ± 0.18 |
| 367 | hfp | 2.13 ± 0.08 | 3.78 ± 0.14 | | | | |

[a] Reference compounds: biphenyl (bp), hexafluoropropene (hfp), fluorene (f), and 3-chlorobiphenyl (pcb2). [b] The errors represent 95% confidence intervals of the mean.

**Rate Constants for the Diphenyl Ether + OH Reaction.** An Arrhenius plot of the rate constants for the reaction of diphenyl ether with OH radicals is shown in Figure 2. The rate constants measured do not show significant temperature dependence, averaging (7.45 ± 0.13) × $10^{-12}$ cm$^3$ molecule$^{-1}$ s$^{-1}$ over the temperature range 326−367 K, where the error represents two standard deviations of the mean; see Tables 2 and 3. Kwok and Atkinson measured the relative rate constant for the diphenyl ether + OH reaction at 297 K in a ∼6500 L Teflon smog chamber using methyl nitrite photolysis as a source of OH radicals.[25] Their value of $k$ (diphenyl ether) = (9.6 ± 2.6) × $10^{-12}$ cm$^3$ molecule$^{-1}$ s$^{-1}$ is 1.3 times higher than our

**TABLE 3: Summary of Rate Constants ($k_4$) for the Gas-Phase Reactions of Diphenyl Ether Derivatives with OH Radicals**

| reactant | $T$ range (K) | $A$ ($10^{-11}$ cm$^3$ molecule$^{-1}$ s$^{-1}$) [a] | $E_a/R$[a] (K) | $k_4$ (298 K)[b] ($10^{-12}$ cm$^3$ molecule$^{-1}$ s$^{-1}$) | $k_{estimate}$ (298 K)[c] ($10^{-12}$ cm$^3$ molecule$^{-1}$ s$^{-1}$) | ref |
|---|---|---|---|---|---|---|
| diphenyl ether | 297 | | | $9.6 \pm 2.6$[d] | | 25 |
| | 326−367 | 1 | 0 | $7.45 \pm 0.13$ | 9.8 | this work |
| 2-bromodiphenyl ether | 326−367 | $2.81^{+0.89}_{-0.68}$ | $533 \pm 96$ | $4.70^{+0.53}_{-0.48}$ | 5.1 | this work |
| 3-bromodiphenyl ether | 326−367 | $8.35^{+4.29}_{-2.83}$ | $863 \pm 142$ | $4.60^{+0.70}_{-0.61}$ | 6.8 | this work |
| 4-bromodiphenyl ether | 326−368 | $0.830^{+0.171}_{-0.142}$ | $109 \pm 65$ | $5.75^{+0.42}_{-0.39}$ | 5.1 | this work |
| 2,2′-dibromodiphenyl ether | 346−378 | $19.8^{+1.0}_{-0.7}$ | $1492 \pm 152$ | $1.33^{+0.31}_{-0.25}$ | 2.1 | this work |
| 2,4-dibromodiphenyl ether | 347−379 | $2.09^{+1.03}_{-0.69}$ | $501 \pm 145$ | $3.88^{+0.87}_{-0.71}$ | 3.6 | this work |
| 3,3′-dibromodiphenyl ether | 346−378 | $8.09^{+3.92}_{-2.64}$ | $960 \pm 142$ | $3.23^{+0.70}_{-0.57}$ | 4.7 | this work |
| 4,4′-dibromodiphenyl ether | 357−388 | $0.0919^{+0.0340}_{-0.0248}$ | $-513 \pm 117$ | $5.14^{+0.98}_{-0.82}$ | 2.1 | this work |
| 2,2′,4,4′,5,5′-hexabromodiphenyl ether | 280 | | | $1.8 \pm 0.9$[d,e] | 0.23 | 13 |

[a] Uncertainties in $A$ and $E_a/R$ are based on one standard error of the intercept and slope from the linear regression to the log-transformed Arrhenius equation. [b] Room-temperature rate constants measured for brominated diphenyl ethers in this work are derived from the Arrhenius equations and are listed with their 95% confidence intervals; our rate constant for diphenyl ether is the average of all rate constants measured within the stated temperature range. [c] Estimates were calculated using the SAR developed by Zetzsch and Kwok and Atkinson.[14,15] The correlation coefficient ($r^2$) between the measurements and these estimates is 0.624, which is significant at $p < 0.05$. [d] Measurements were made at the single temperature indicated; errors are as quoted by the authors. [e] Measured adsorbed on silica particles.

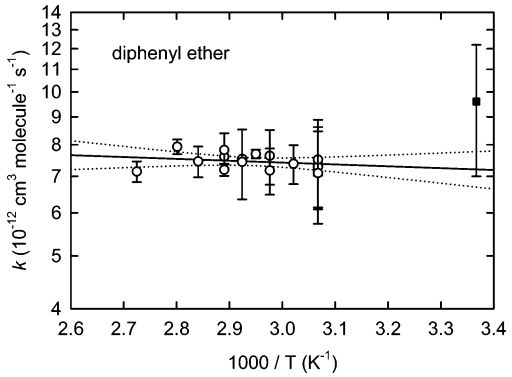


**Figure 2.** Arrhenius plot for the reaction of diphenyl ether with OH radicals. Data from the present study (○) and the value previously measured by Kwok and Atkinson at 297 K[25] (■); error bars represent the 95% confidence limit of the mean of each measurement: lines, (—) regression; (···) 95% confidence limits of the regression.

measured OH rate constant at 298 K, although the two values agree with each other within the estimated uncertainties. In their relative rate experiments, Kwok and Atkinson detected diphenyl ether and a reference compound (cyclohexane) by gas chromatography with flame ionization detection. Diphenyl ether was periodically collected from the smog chamber onto Tenax-TA solid adsorbent followed by thermal desorption onto the GC column; cyclohexane was sampled in gastight syringes and transferred to the GC. It is unclear whether these disparate sampling techniques could lead to an error in the rate constant measurement.

There are two reasons that the rate constant for diphenyl ether could be artificially low in our experiments: (1) the reference compound decays (via secondary reactions or photolysis) faster than it would from OH reactions alone or (2) an unknown product grows in during the reaction and shares $m/z$ values with diphenyl ether. Photolysis of the reference compound (biphenyl) can be discounted based on control experiments performed in the absence of $i$-$C_3H_7ONO$ (biphenyl does not absorb UV light >290 nm). Control experiments performed in the absence of diphenyl ether indicate that the reference compounds, biphenyl and $C_3F_6$, do not produce products having $m/z$ values in common with diphenyl ether. Moreover, the linearity of the relative rate plots (at least over 2 min) suggests that products of the diphenyl ether + OH reaction do not contribute to the measured decays.

It should be noted that ozone, from $NO_2$ photolysis in the presence of oxygen, is known to interfere with OH rate determinations for systems where alkyl nitrites are used as OH radical sources. Ozone was not detected via mass spectrometry for any experiment during the photolysis of $i$-$C_3H_7ONO$, although this is not conclusive proof of its absence because the detection limit was high as a result of a high background signal at $m/z$ 48. No difference in diphenyl ether + OH rate constants was observed in the presence or absence of added NO ($\sim 10^{13}$ molecules cm$^{-3}$), suggesting that the measured rate constants are likely unaffected by the presence of small quantities of ozone. The room-temperature rate constant for the reaction of diphenyl ether with $O_3$ is expected to be $< 2 \times 10^{-20}$ cm$^3$ molecule$^{-1}$ s$^{-1}$, similar to gas-phase rate constants for the reaction of $O_3$ with structurally related compounds such as polychlorinated biphenyls (PCBs) and polychlorinated dibenzo-$p$-dioxins/dibenzofurans (PCDD/Fs).[7] Hence, small amounts of ozone would likely not contribute to the observed decay of diphenyl ether (or brominated diphenyl ethers).

**Rate Constants for PBDE + OH Reactions.** Measurements of OH rate constants were conducted for the brominated diphenyl ethers listed in Table 1 over the temperature range of 326−388 K for the purpose of deriving room-temperature rate constants by extrapolation and identifying trends in reactivity among the different congeners. Arrhenius plots of the three monobrominated diphenyl ethers and four dibrominated diphenyl ethers are shown in Figures 3 and 4; Arrhenius parameters are presented in Table 3.

The rate constants for most PBDEs show positive temperature dependences corresponding to values of $E_a/R$ in the Arrhenius expression ranging from $109 \pm 65$ for 4-bromodiphenyl ether to $1492 \pm 152$ for 2,2′-dibromodiphenyl ether. The exception was 4,4′-dibromodiphenyl ether ($E_a/R = -513 \pm 117$), which was the only congener studied to show an increase in rate constants with decreasing temperature. Positive dependences of rate constants on temperature have also been observed for the reactions of OH with PCBs,[17] PCDDs,[18,26] halogenated benzenes,[27−30] and tetrachloroethylene.[31]

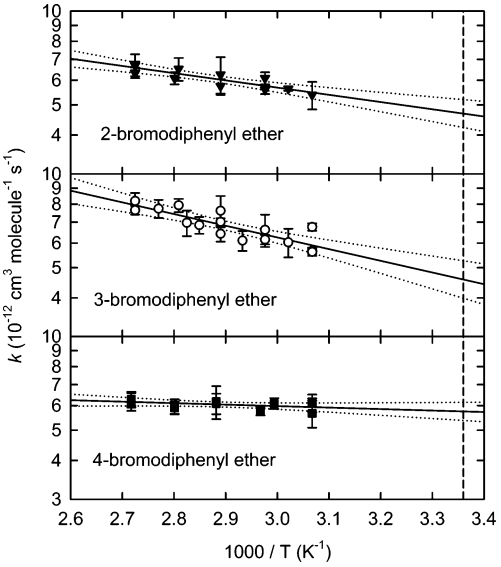


**Figure 3.** Arrhenius plots for the reaction of the indicated monobrominated diphenyl ethers with OH radicals; error bars represent the 95% confidence limit of the mean of each measurement: lines, (—) regression; (•••) 95% confidence limits of the regression; (- - -) $T$ = 298 K.

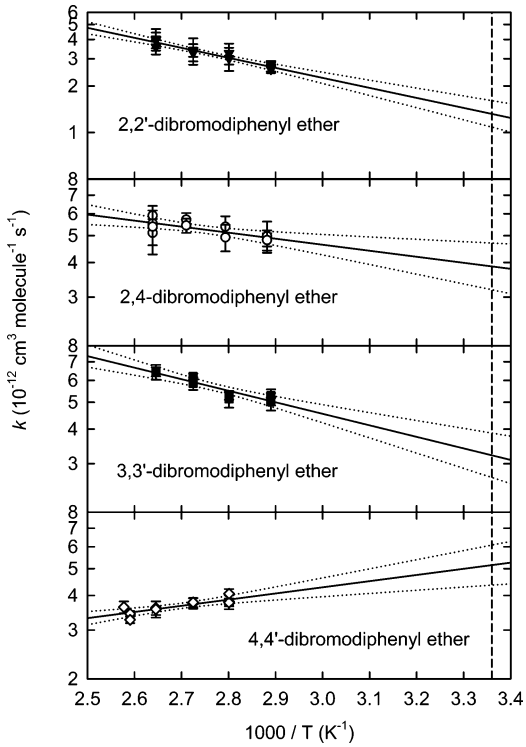


**Figure 4.** Arrhenius plots for the reaction of the indicated dibrominated diphenyl ethers with OH radicals; error bars represent the 95% confidence limit of the mean of each measurement: lines, (—) regression; (•••) 95% confidence limits of the regression; (- - -) $T$ = 298 K.

Table 3 also includes the room-temperature rate constants for the brominated diphenyl ethers studied here and the OH rate constant measured for 2,2′,4,4′,5,5′-hexabromodiphenyl ether (BDE-153) adsorbed to $SiO_2$ aerosols at 280 K.[13] In general, the rate constants for diphenyl ether derivatives decrease with increasing bromination, an effect related to the reduction of electron density on the phenyl rings by the bromine substituents. There is a further dependence of the OH rate constants on the substitution pattern. For example, PBDEs with unoccupied sites ortho to the O atom are most reactive, while ortho substitution with bromine appears to reduce the reactivity (compare 4,4′- vs 2,2′-dibromodiphenyl ether). In this case, the phenoxy group donates electron density to the aromatic ring and activates the positions ortho to the O atom toward electrophilic addition. This is consistent with the studies of the reactions of OH with phenol and cresol isomers, where positions ortho to the hydroxy group are activated and 1,2-dihydroxybenzenes are the dominant products.[32,33]

The delocalization of electron density over the diphenyl ether backbone may also contribute to differences in reactivity between PBDE congeners. In particular, conjugation of the two aryl rings in diphenyl ether occurs over the ether oxygen and depends on the steric and electron-accepting/donating properties of the attached substituents. It has been shown that diphenyl ethers with electron-withdrawing groups (e.g., cyano, ester, acyl, and nitro) in para positions adopt a conformation in which the bridging oxygen $\pi$-lone-pair conjugates with the $\pi$-electron system of the two rings.[34] Evidence of this behavior is also found in the solution-phase absorption spectra of PBDEs, where the lowest energy absorption band of 4,4′-dibromodiphenyl ether is red shifted by almost 10 nm relative to the 2,2′- and 3,3′-substituted congeners. The added electron delocalization would result in an elevated HOMO (reducing the HOMO−LUMO gap) in para-substituted diphenyl ethers relative to ortho- and meta-substituted congeners and may also contribute to the increased reactivity observed for 4-bromodiphenyl ether and 4,4′-dibromodiphenyl ether, compared with the analogous ortho- and meta-substituted congeners.

Table 3 also compares our experimentally determined rate constants with those estimated from the SAR developed by Kwok and Atkinson[15] and Zetzsch,[14] using the electrophilic subsituent constants of Brown and Okamoto.[35] The SAR predicts reasonably well (within a factor of 2) the trends of OH rate constants for PBDEs congeners based on bromination level. However, it falls short in predicting how reactivity depends on the substitution pattern within a congener class. This is particularly evident in the discrepancy between experimental and predicted rate constants for congeners with meta and para substitution. The SAR method predicts aromatic compounds with halogens in meta positions to be most reactive, while ortho and para substitution leads to lower reactivity. Exactly the opposite is seen in the experimental measurements for PBDEs. These differences may not be surprising considering that the SAR method is based on correlations of OH rate coefficients and electrophilic substituent constants for simple monocyclic aromatic hydrocarbons.

The only published example of PBDE−OH reactivity is the study by Zetzsch et al.[13] In this smog chamber experiment, 2,2′,4,4′,5,5′-hexabromodiphenyl ether (BDE-153) was reacted with OH radicals while adsorbed to $SiO_2$ aerosols at 280 K.[13] The absolute rate constant measured for the reaction of OH with BDE-153 is almost 8 times faster than the rate constant predicted by the SAR method ($k_{est}$ (BDE-153) = $0.23 \times 10^{-12}$ cm$^3$ molecule$^{-1}$ s$^{-1}$). The discrepancy between the predicted and measured rate constant could stem from an enhancement of the OH rate constant mediated by the surface of the aerosol, although this aerosol−smog chamber method has in the past provided reasonable estimates of gas-phase reactivity.[36] In addition, a recent study by Sørensen et al. has shown that the presence of pure-phase aerosols (e.g., NaCl, $(NH_4)_2SO_4$, or $NH_4NO_3$) in smog chamber experiments did not enhance the rate of reaction between OH and some volatile organic compounds.[37] At this point, there remains some uncertainty whether the decay

of BDE-153 observed in this chamber study was due solely to OH radicals. Additional smog chamber experiments would be useful to resolve the discrepancy.

**Mechanism of OH + PBDE Reactions.** The temperature dependence of the OH rate constants reveals information about the mechanism of the reaction of OH radicals with diphenyl ether derivatives. Arrhenius plots of diphenyl ether and 4,4′-dibromodiphenyl ether suggest that reactions of these molecules with OH radicals occur via transition states having energies that are equal to or less than the energy of the reactant states, similar to what is observed for other PAHs.[7] In these cases, OH radicals would react reversibly via an addition reaction to the aromatic ring, forming a vibrationally excited diphenyl ether−OH* adduct that is stabilized by the diluent gas and subsequently reacts with oxygen to form products (reactions 10−12).

$$\text{diphenyl ether} + \text{OH} \leftrightarrow \text{diphenyl ether radical}-\text{OH}^* \quad (10)$$

$$\text{diphenyl ether radical}-\text{OH}^* + \text{M} \rightarrow \text{diphenyl ether radical}-\text{OH} + \text{M}^* \quad (11)$$

$$\text{diphenyl ether radical}-\text{OH} + \text{O}_2 \rightarrow \text{products} \quad (12)$$

The negative temperature dependence observed for 4,4′-dibromodiphenyl ether would indicate that collisional processes, which are more important at the lower temperatures, are necessary to stabilize the OH addition adduct in reaction 10. Interestingly, the temperature dependence of 4-bromodiphenyl ether is almost thermoneutral compared with the other bromodiphenyl ethers. This suggests that 4-bromodiphenyl ether may share a reaction mechanism in common with diphenyl ether and 4,4′-dibromodiphenyl ether or at least that reactions 10−12 may play a more important role in the reaction of OH radicals with 4-bromodiphenyl ether.

There is an additional consideration in the discussion of OH + PBDE reaction mechanisms: the possibility of hydrogen bonding. Studies on the reactivity of alkyl ethers with OH radicals have provided evidence for the existence of a cyclic hydrogen-bonded complex involving an OH radical, the ether O atom, and an adjacent methylene group.[38,39] This pre-reactive complex is thought to reduce the activation energy of the reaction and lead to the negative temperature dependences observed for the more reactive ethers. In the case of diphenyl ethers, a six-membered hydrogen-bonded complex may form upon interaction of the attacking OH radical with the O atom of the diphenyl ether and a hydrogen atom in a position ortho to the oxygen on the aryl ring; a bromine atom at an ortho position would sterically block this interaction:

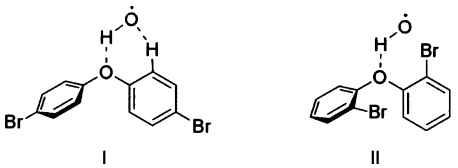


(13)

This may explain the enhanced reactivity and temperature dependences observed for diphenyl ether, 4-bromodiphenyl ether, and 4,4′-dibromodiphenyl ether because hydrogen bond formation is an associative process that would be favored at lower temperatures.

The positive temperature dependence observed for all the other PBDEs studied suggests the presence of a barrier on the potential energy surface that is indicative of a more complicated reaction mechanism. A positive temperature dependence is usually observed for OH + hydrocarbon reactions where H-abstraction is the dominant reaction pathway. However, it is unlikely that H-abstraction from PBDEs occurs, given that abstraction of hydrogen from halogenated aromatics only becomes important at higher temperatures.[7,28] In fact, the onset temperature of H-atom abstraction from aryl rings has been shown to depend on the number and identity of halogen substituents, shifting to higher temperatures with the number of halogen substituents or as the identity of the substituent progresses from fluorine to iodine.[28]

Abstraction of bromine atoms from PBDEs to form diphenyl ether radicals and HOBr could also be considered as another explanation of the positive temperature dependence:

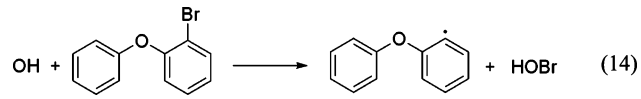


(14)

However, this reaction mechanism is not likely based on the following thermodynamic arguments. By taking the heats of formation of reactants and products to be $\Delta H_f$ (BDE-1) = 82 kJ mol$^{-1}$,[40] $\Delta H_f$ (OH) = 38 kJ mol$^{-1}$,[41] $\Delta H_f$ (diphenyl ether radical) = 292 kJ mol$^{-1}$,[42] and $\Delta H_f$ (HOBr) = −61 kJ mol$^{-1}$,[41] the reaction enthalpy of reaction 14 is determined to be endothermic by 111 kJ mol$^{-1}$.

Within the temperature ranges investigated in this study, reactions of PBDEs with OH likely occur via OH-addition. The addition of OH to an unsubstituted position in a PBDE may proceed via pathways analogous to reactions 10−12, while addition to ipso positions may involve competition between adduct stabilization and bromine or phenoxy radical elimination:

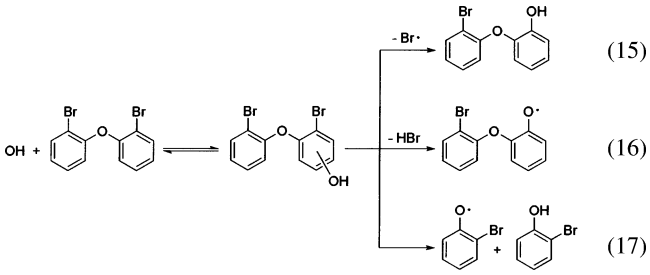


Enthalpy of formation values for most of the products outlined in reactions 15−17 are unavailable, making it impossible to assess the thermodynamic feasibility of these reactions. There is some indication that halogen displacement occurs to some extent in gas-phase reactions of halogenated aryls with electrophilic radicals. A halogen loss mechanism has been proposed to play a role in the reaction of OH radicals with chlorinated benzenes.[43] Chlorine atoms, which are often used as surrogates for OH radicals to initiate photooxidation reactions, have been shown to displace other halogens in fluoro-, bromo-, and iodobenzene.[44−46] However, it should be pointed out that Nakano et al. failed to observe the displacement product, phenol, during the reaction of OH with bromobenzene (<10% yield).[46] A chlorine elimination mechanism is also known to play an important role in the addition of OH to chloroethylenes.[31,47]

The addition of OH to an ipso-O position has no precedence in the gas-phase literature on aryl + OH reactions, although it is observed commonly in the solution phase.[48−52] Addition to the ipso position has been suggested as a possible reaction pathway in the gas-phase reaction of phenol with $NO_3$.[53,54] A few computational studies have been carried out to investigate the feasibility of OH-addition to the ipso position of substituted aromatic hydrocarbons. In particular, OH-addition to methylated benzenes has been investigated using unrestricted Hartree−Fock

methods[55] or density functional theory.[56] In these cases, ipso-substituted OH-adducts were found to be less stable than ortho-substituted isomers, although the energy differences were within the uncertainties of the calculations.

**Product Studies.** Products from the PBDE + OH reaction were identified by gas chromatographic mass spectrometry (GC/MS) after they were extracted from the reaction chamber walls with organic solvents. In separate experiments, 4-bromodiphenyl ether, 2,2′-dibromodiphenyl ether, and 2,4-dibromodiphenyl ether were reacted for 10−30 min with OH radicals at 346 K. In all cases, hydrogen peroxide photolysis at $\lambda \geq 320$ nm provided OH radicals in low concentrations ([OH] = $1-5 \times 10^7$ molecules $cm^{-3}$) in an attempt to minimize secondary reactions. GC/MS analysis of the reactor extracts revealed the presence of small quantities of brominated phenols (6−20% relative to the amount of PBDE reacted) as the only brominated products present in the extracts. The identities of the phenols formed in these experiments were confirmed by comparison of their mass spectra and gas chromatographic retention times to those from authentic samples. In each experiment, the identity of the phenol corresponded in substitution pattern to the diphenyl ether reactant. Hence, 4-bromophenol, 2-bromophenol, and 2,4-bromophenol were identified from the reaction of OH with 4-bromodiphenyl ether, 2,2′-dibromodiphenyl ether, and 2,4-dibromodiphenyl ether, respectively.

Several experiments were also performed using *i*-$C_3H_7ONO$ photolysis as a source of OH. In these cases, nitrobromophenols were detected as minor products (~6% relative to the amount of PBDE consumed) in reactor extracts. However, it was subsequently determined that nitration of bromophenols likely occurred during extraction and analysis rather than photochemically in the gas-phase (probably from the presence of $HNO_3$ on the reactor walls or in the extracts). Several extracts were also derivitized with diazomethane in an effort to detect additional polar products. Hydroxylated PBDEs were detected as their methylated derivatives infrequently and only in trace amounts; the identification of these compounds was based solely on interpretation of their EI mass spectra due to the lack of authentic samples. Under the relatively high OH radical concentrations used in these experiments, hydroxydiphenyl ethers are likely consumed by secondary reactions with OH radicals as soon as they are produced; for example, the predicted OH rate constant of 2-hydroxy-2′-bromodiphenyl ether is ~6 times faster than that of 2-bromodiphenyl ether.

The observation of brominated phenols as reaction products suggests that OH addition to the ipso-O position on a PBDE (reaction 17) is a potentially viable reaction mechanism, although it is unclear whether this reaction occurs as a gas- or heterogeneous-phase reaction. The addition of OH to an ipso-O position has been observed in solution-phase ($H_2O$, acetonitrile) reactions of OH radicals with various aromatics containing phenoxy moieties.[48−52] The most relevant example comes from Matsuura et al. who found that phenols were formed in yields around 20% from the reaction of thyropropionic acid (a diphenyl ether containing hydroxy- and propionic acid groups in para positions) with OH radicals generated by photodecomposition of $H_2O_2$ in water or acetonitrile.[48] Hence, it is possible that the phenolic products observed here are formed by the reaction of OH with PBDEs in the condensed phase on the reactor walls.

Online product analysis was carried out by collecting full-scan mass spectra of the reaction cell contents recorded after various PBDE + OH reactions had proceeded to 50% completion. Molecular bromine was detected for all PBDE reactions monitored, as indicated by the presence of ions at *m*/*z* 158, 161, and 162 with relative intensities of 1:2:1. Figure 5a shows the evolution of $Br_2$ during the reaction of 2,2′-dibromodiphenyl ether with OH. The bromine signal in this experiment follows a first-order exponential rise to a maximum, and the ratio of the rate constant for 2,2′-dibromodiphenyl ether loss to bromine formation is 1.5. It is important to note that $Br_2$ was only detected in reaction mixtures when OH radicals were generated in the presence of PBDEs, suggesting that OH radicals are directly or indirectly responsible for $Br_2$ formation.

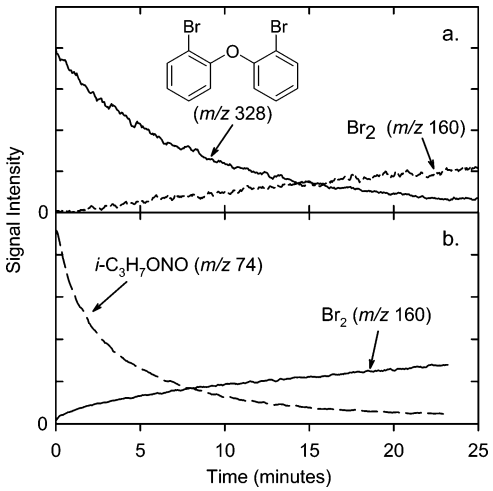


**Figure 5.** (a) Loss of 2,2′-dibromodiphenyl ether and formation of $Br_2$ at 70 °C during the photolysis of *i*-$C_3H_7ONO$ in He/Air mixture at ~740 Torr. (b) Formation of $Br_2$ at 70 °C from the heterogeneous reaction of OH radicals (from *i*-$C_3H_7ONO$ photolysis) and NaBr adsorbed to the surface of the quartz reactor walls.

There are several possible sources of $Br_2$ in our reaction system. Bromine atoms may be released during a displacement reaction (reaction 15) and could recombine in the gas phase or on reactor walls. Secondary reactions of OH radicals with bromine-containing reaction products could release molecular bromine, as well. Recent studies of air−sea salt interfacial processes have shown that the heterogeneous reactions of OH radicals with bromide ions in aerosols are a source of $Br_2$ at the troposphere−marine boundary layer.[57,58] If OH + PBDE reactions proceeded to some extent via reaction 16, or if HBr was generated in secondary reactions with reaction products, the heterogeneous reaction of $Br^-$ with OH could be a source of $Br_2$ in the reactor. Indeed, formation of $Br_2$ was observed when He/air/*i*-$C_3H_7ONO$ mixtures were photolyzed in a reaction chamber whose walls had previously been coated with a 0.05 M solution of NaBr; see Figure 5b. Incidentally, Br atoms generated during our kinetic experiments probably do not contribute to the observed photochemical loss of PBDEs, since Br atoms react very slowly ($<10^{-14}$ $cm^3$ $molecule^{-1}$ $s^{-1}$) with aromatic hydrocarbons.[59]

**Atmospheric Implications.** The atmospheric lifetimes ($\tau$) of the PBDEs based on reactions with OH radicals may be estimated from $\tau = 1/k_{OH}$ [OH], using room-temperature OH rate constants ($k_{OH}$) and an average global OH concentration of $9.7 \times 10^5$ molecules $cm^{-3}$, derived from measurements of methyl chloroform abundances.[60] The atmospheric lifetimes of mono- and dibrominated PBDEs studied here are calculated to be between 2−2.6 and 2.3−3.7 days, respectively. By the use of SAR predicted OH rate constants, lifetimes for PBDEs range from 3 days for tribrominated diphenyl ethers to 46 days for some hexabrominated diphenyl ethers. Congeners with 6 or more bromines are found predominantly (>70%) in the particle phase,[61] and their observed reactivity may not follow gas-phase reactivity patterns owing to additional physical and chemical

considerations that are unique to the particle phase. On the basis of these estimates, gas-phase PBDEs having more than three bromines are likely to undergo atmospheric transport to regions far removed from their sources. Processes such as photolysis, wet and dry deposition, and reaction with $NO_3$ radicals may also shorten the atmospheric lifetimes of PBDEs, although the contributions of these loss pathways have yet to be determined.

**Acknowledgment.** This research has been funded in part by the United States Environmental Protection Agency (EPA) under the Science to Achieve Results (STAR) Graduate Fellowship Program (FP-91663501). EPA has not officially endorsed this publication, and the views expressed herein may not reflect those of the EPA. Additional funding comes from the Atmospheric Chemistry section of the National Science Foundation (Grant ATM-0106705). The authors are grateful to Drs. Philip Stevens and Sebastien Dusanter for helpful discussions and to the Hamamatsu Corporation for their donation of the Hg−Xe arc lamp used in these studies. We also thank an anonymous reviewer whose insightful comments helped improve this paper.

## References and Notes

(1) Hites, R. A. *Environ. Sci. Technol.* **2004**, *38*, 945−956.

(2) Hoh, E.; Hites R. A. *Environ. Sci. Technol.* **2005**, *39*, 7794−7802.

(3) Wang, X.-M.; Ding, X.; Mai, B.-X.; Xie, Z.-Q.; Xiang, C.-H.; Sun, L.-G.; Sheng, G.-Y.; Fu, J.-M., Zeng, E. Y. *Environ. Sci. Technol.* **2005**, *39*, 7803−7809.

(4) See, for example: Thomsen, C.; Lundanes, E.; Becher, G. *Environ. Sci. Technol.* **2002**, *36*, 1414−1418. Wolkers, H.; Van Bavel, B.; Derocher, A. E.; Wiig, Ø.; Kovacs, K. M.; Lydersen, C.; Lindström, G. *Environ. Sci. Technol.* **2004**, *38*, 1667−1674. Lebeuf, M.; Gouteux, B.; Measures, L.; Trottier, S. *Environ. Sci. Technol.* **2004**, *38*, 2971−2977.

(5) Ikonomou, M. G.; Rayne, S.; Addison, R. F. *Environ. Sci. Technol.* **2002**, *36*, 1886−1892.

(6) For reviews of PBDE toxicology, see: Birmbaum, L. S.; Staskak, D. F. *Environ. Health Perspect.* **2004**, *112*, 9−17. Legler, J.; Brouwer, A. *Environ. Int.* **2003**, *29*, 879−885.

(7) Calvert, J. G.; Atkinson, R.; Becker, K. H.; Kamens, R. M.; Seinfeld, J. H.; Wallington, T. J.; Yarwood, G. *The Mechanisms of Atmospheric Oxidation of Aromatic Hydrocarbons*; Oxford University Press: New York, 2002.

(8) Hua, I.; Kang, N.; Jafvert, C. T.; Fábrega-Duque, J. *Environ. Toxicol. Chem.* **2003**, *22*, 798−804.

(9) Söderström, G.; Sellström, U.; de Wit, A. C.; Tysklind, M. *Environ. Sci. Technol.* **2004**, *38*, 127−132.

(10) Eriksson, J.; Green, N.; Marsh, G.; Bergman, Å. *Environ. Sci. Technol.* **2004**, *38*, 3119−3125.

(11) Bezares-Cruz, J.; Jafvert, C. T.; Hua, I. *Environ. Sci. Technol.* **2004**, *38*, 4149−4156.

(12) Ahn, M.-Y.; Filley, T. R.; Jafvert, C. T.; Nies, L.; Hua, I.; Bezares-Cruz, J. *Environ. Sci. Technol.* **2006**, *40*, 215−220.

(13) Zetzsch, C.; Palm, W.-U.; Krüger, H.-U. *Organohalogen Compd.* **2004**, *66*, 2281−2287.

(14) Zetzsch, C. In *Predicting the Rate of OH-Addition to Aromatics using $\sigma^+$-Electrophilic Substituent Constants for Mono- and Polysubstituted Benzene*, Proceedings of the 15th Informal Conference on Photochemistry; Slanger, T., Golden, D. M., Eds.; Stanford, CA, 1982; pp 29−32.

(15) Kwok, E. S. C.; Atkinson, R. *Atmos. Environ.* **1995**, *29*, 1685−1695.

(16) Anderson, P. N.; Hites, R. A. *Environ. Sci. Technol.* **1996**, *30*, 301−306.

(17) Anderson, P. N.; Hites, R. A. *Environ. Sci. Technol.* **1996**, *30*, 1756−1763.

(18) Brubaker, W. W.; Hites, R. A. *J. Phys. Chem. A* **1998**, *102*, 915−921.

(19) Lee, W.; Stevens, P. S.; Hites, R. A. *J. Phys. Chem. A* **2003**, *107*, 6603−6608.

(20) Raff, J. D.; Stevens, P. S.; Hites, R. A. *J. Phys. Chem. A* **2005**, *109*, 4728−4735.

(21) Rate constants for the reaction of biphenyl with OH have only been determined within the temperature range 294−356 K. It was therefore necessary to determine the rate constants for the biphenyl + OH reaction at 107 °C, the highest temperature for which biphenyl was used. Through the use of the relative rate method discussed above (with hydrogen peroxide photolysis at $\lambda \geq 254$ nm as the OH source and cyclohexane as a reference compound), a value of $(7.3 \pm 0.4) \times 10^{-12}$ cm$^3$ molecule$^{-1}$ s$^{-1}$ was determined, where quoted uncertainties are two standard deviations of the mean from three separate experiments. The excellent agreement of this value with those measured at lower temperatures suggests that the previous recommendation by Calvert et al.[7] is valid up to 380 K.

(22) Tokuhashi, K.; Takahashi, A.; Kaise, M.; Kondo, S.; Sekiya, A.; Fujimoto, E. *Chem. Phys. Lett.* **2000**, *325*, 189−195.

(23) Black, T. H. *Aldrichimica Acta* **1983**, *16*, 3−10.

(24) Finlayson-Pitts, B. J.; Wingen, L. M.; Sumner, A. L.; Syomin, D.; Ramazan, K. A. *Phys. Chem. Chem. Phys.* **2003**, *5*, 223−242.

(25) Kwok, E. S. C.; Atkinson, R.; Arey, J. *Environ. Sci. Technol.* **1995**, *29*, 1591−1598.

(26) Brubaker, W. W.; Hites, R. A. *Environ. Sci. Technol.* **1998**, *32*, 766−769.

(27) Witte, F.; Urbanik, E.; Zetzsch, C. *J. Phys. Chem.* **1986**, *90*, 3251−3259.

(28) Wallington, T. J.; Neuman, D. M.; Kurylo, M. J. *Int. J. Chem. Kinet.* **1987**, *19*, 725−739.

(29) McIlroy, A.; Tully, F. P. *J. Phys. Chem.* **1993**, *97*, 610−614.

(30) Brubaker, W. W.; Hites, R. A. *Environ. Sci. Technol.* **1997**, *31*, 1805−1810.

(31) Tichenor, L. B.; Graham, J. L.; Yamada, T.; Taylor, P. H.; Peng, J.; Hu, X.; Marshall, P. *J. Phys. Chem. A* **2000**, *104*, 1700−1707.

(32) Olariu, R. I.; Klotz, B.; Barnes, I.; Becker, K. H.; Mocanu, R. *Atmos. Environ.* **2002**, *36*, 3685−3697.

(33) Berndt, T.; Böge, O. *Phys. Chem. Chem. Phys.* **2003**, *5*, 342−350.

(34) Uno, B.; Iwamoto, T.; Okumura, N. *J. Org. Chem.* **1998**, *63*, 9794−9800.

(35) Brown, H. C.; Okamoto, Y. *J. Am. Chem. Soc.* **1958**, *80*, 4979−4987.

(36) See, for example: Behnke, W.; Nolting, F.; Zetzsch, C. *J. Aerosol Sci.* **1987**, *18*, 849−852. Palm, W.-U.; Elend, M.; Krüger, H.-U.; Zetzsch, C. *Environ. Sci. Technol.* **1997**, *66*, 33389-3396.

(37) Sørensen, M.; Hurley, M. D.; Wallington, T. J.; Dibble, T. S.; Nielsen, O. J. *Atmos. Environ.* **2002**, *36*, 5947−5947.

(38) Porter, E.; Wenger, J.; Treacy, J.; Sidebottom, H.; Mellouki, A.; Téton, S.; Le Bras, G. *J. Phys. Chem. A* **1997**, *101*, 5770−5775.

(39) Moriarty, J.; Sidebottom, H.; Wenger, J.; Mellouki, A.; Le Bras, G. *J. Phys. Chem. A* **2003**, *107*, 1499−1505.

(40) Zeng, X.; Freeman, P. K.; Vasil'ev, Y. V.; Voinov, V. G.; Simonich, S. L.; Barofsky, D. F. *J. Chem. Eng. Data* **2005**, *50*, 1548−1556.

(41) Sander, S. P.; Ravishankara, A. R.; Friedl, R. R.; Golden, D. M.; Kolb, C. E.; Kurylo, M. J.; Molina, M. J.; Huie, R. E.; Orkin, V. L.; Moortgat, G. K.; Finlayson-Pitts, B. J. *Chemical Kinetics and Photochemical Data for Use in Atmospheric Studies*; Technical Report, Evaluation Number 14; Jet Propulsion Laboratory: Pasadena, CA, 2003.

(42) Afeefy, H. Y.; Liebman, J. F.; Stein, S. E. In *Neutral Thermochemical Data*; NIST Chemistry WebBook, NIST Standard Reference Database Number 69; Linstrom, P. J., Mallard, W. G., Eds.; June 2005, National Institute of Standards and Technology: Gaithersburg, MD, 20899 (http://webbook.nist.gov).

(43) Wahner, A.; Zetzsch, C. *J. Phys. Chem.* **1983**, *87*, 4945−4951.

(44) Sulbaek Andersen, M. P.; Nielsen, O. J.; Hurley, M. D.; Wallington, T. J. *J. Phys. Chem. A* **2002**, *106*, 7779−7787.

(45) Sulbaek Andersen, M. P.; Ponomarev, D. A.; Nielsen, O. J.; Hurley, M. D.; Wallington, T. J. *Chem. Phys. Lett.* **2001**, *350*, 423−426.

(46) Nakano, Y.; Ponomarev, D. A.; Hurley, M. D.; Wallington, T. J. *Chem. Phys. Lett.* **2002**, *353*, 77−83.

(47) Canosa-Mas, C. E.; Dillon, T. J.; Sidebottom, H.; Thompson, K. C.; Wayne, R. P. *Phys. Chem. Chem. Phys.* **2001**, *3*, 542−550.

(48) Matsuura, T.; Nagamachi, T.; Nishinaga, A. *J. Org. Chem.* **1971**, *36*, 2016−2017.

(49) Quint, R. M.; Park, H. R.; Krajnik, P.; Solar, S.; Getoff, N.; Sehested, K. *Radiat. Phys. Chem.* **1996**, *47*, 835−845.

(50) Schuler, R. H.; Albarran, G.; Zajicek, J.; George, M. V.; Fessenden, R. W.; Carmichael, I. *J. Phys. Chem. A* **2002**, *106*, 12178−12183.

(51) Albarran, G.; Schuler, R. H. *J. Phys. Chem. A* **2005**, *109*, 9363−9370.

(52) Peller, J.; Wiest, O.; Kamat, P. V. *J. Phys. Chem. A* **2004**, *108*, 10925−10933.

(53) Bolzacchini, E.; Bruschi, M.; Hjorth, J.; Meinardi, S.; Orlando, M.; Rindone, B.; Rosenbohm, E. *Environ. Sci. Technol.* **2001**, *35*, 1791−1797.

(54) Harrison, M. A. J.; Barra, S.; Borghesi, D.; Vione, D.; Arsene, C.; Olariu, R. I. *Atmos. Environ.* **2005**, *39*, 231−248.

(55) Bolzacchini, E.; Bruschi, M.; Hjorth, J.; Meinardi, S.; Orlandi, M.; Reselli, G.; Rindone, B. In *Tropospheric chemistry of aromatic compounds: Evidence for a rate-determining addition of $NO_3$ and OH to substituted toluenes*, Proceedings of the 5th International Conference on Air Pollution: Modeling, Monitoring and Management, Bologna, Italy, 1997; pp 893−902.

(56) Johnson, D.; Raoult, S.; Lesclaux, R.; Krasnoperov, L. N. *J. Photochem. Photobiol., A* **2005**, *176*, 98−106.

(57) Anastasio, C.; Mozurkewich, M. *J. Atmos. Chem.* **2002**, *41*, 135−162.
(58) Thomas, J. L.; Jimenez-Aranda, A.; Finlayson-Pitts, B. J.; Dabdub, D. *J. Phys. Chem. A* **2006**, *110*, 1859−1867.
(59) Bierbach, A.; Barnes, I.; Becker, K. H. *Int. J. Chem. Kinet.* **1996**, *28*, 565−577.
(60) Prinn, R. G.; Weiss, R. F.; Miller, B. R.; Huang, J.; Alyea, F. N.; Cunnold, D. M.; Fraser, P. J.; Hartley, H. E.; Simmonds, P. G. *Science* **1995**, *259*, 187−192.
(61) Chen, L.-G.; Mai, B.-X.; Bi, X.-H.; Chen, S.-J.; Wang, X.-M.; Ran, Y.; Luo, X.-J.; Sheng, G.-Y.; Fu, J.-M., Zeng, E. Y. *Environ. Sci. Technol.* **2006**, *40*, 1190−1196.